RSC Advances

ROYAL SOCIETY OF CHEMISTRY

www.rsc.org/advances

Cite this: DOI: 10.1039/c0xx00000x

www.rsc.org/advances

PAPER

Synthesis of 4-phenyl-5,6-dihydrobenzo[*h*]quinazolines and their evaluation as growth inhibitors of carcinoma cells

Hardesh K Maurya[a], Mohammad Hasanain[d], Sarita Singh[a], Jayanta Sarkar[d], Vijaya Dubey[b], Aparna Shukla[c], Suaib Luqman[b], Feroz Khan,[c] Atul Gupta[a,#]*

Synthesis of various benzo[*h*]quinazoline analogs (**4a-f, 6a-6d** and **8a-b**) was accomplished through the reaction of chalcone with guanidine. The synthesized compounds (**4a-f, 6a-6d & 8a-b**) were screened for their anticancer potential against different cancer cells *viz* MCF-7, DLD1, A549, Du145 & FaDu cell lines. Compounds **4a**, **6a-d** & **8b** showed significant anticancer activity in these cancer cell lines within the range of IC_{50} values of 1.5-12.99 µM. Functional study of a promising molecule, **6d,** at 7 µM **(**at IC_{50} value**)** for 24 and 48 h showed that it possessed anticancer activity through triggering apoptosis. In tubulin polymerization assay, **6d** effectively inhibited tubulin polymerization at IC_{50} 2.27 µM. *In-silico* docking study of **6d** revealed that **6d** had good affinity with estrogen receptor as well as tubulin protein on its β-sheet of colchicines binding site.

Introduction

Any defect in programmed cell growth of a normal healthy cell leads to accumulation of undesired defective cells and ultimately develop Cancer. Cancer is a leading cause of death worldwide. The present statistics revealed that it accounts for one in every seven deaths globally which is more than any other infectious disease.[1] By 2030, it is expected that about 21.7 million new cancer cases and 13.0 million cancer deaths will be reported.[2] Lung, prostate, colorectum, stomach, and liver cancers are very common in males while in females stomach, breast, uterine and cervix cancers are frequent and the common cause of cancers is imbalance in hormone.[3] Among several other estrogen-dependent cancers, breast cancer is a leading pandemic that affects women over a wide age group.[3] Considering the necessity of the anticancer chemotherapeutics for treatment of estrogen dependent cancers such as breast cancer, different estrane based molecules such as fulvestrant (ICI-182,780, **I**), ICI-164,384 (**II**), SR-16157 (**IV**), SR-16234 (**V**), 3-hydroxy-estra-1,3,5(10)trien-17-oxo-15β-morpholinobutan-1-one (**VI**), estradiol-chlorambucil conjugates (**VI**), estra-13,5(10)-trien-16,17 [3,4]- pyrazolo-N-(3-ehtylpyridino)-5-caboxamide (**VII**), VP-128 (**VIII**), 16α,β-[11-(2-pyridylethylamino)undecanyl]-estradiol dichloroplatium (II) complexes (**IX**) have been discovered with potent anti-breast cancer potential, Figure 1.[4-11] It is reported that estrogen receptor-α (ER-α) dominates in breast cancer tissue and is the main culprit for excess cell proliferation.

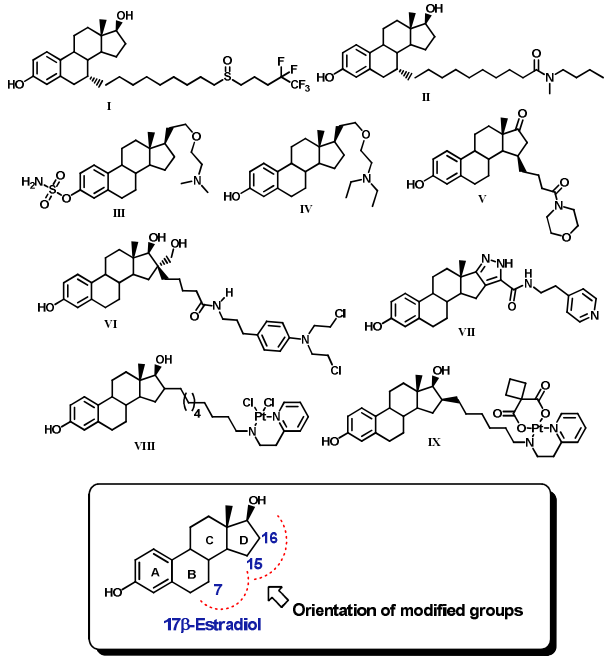

Fig. 1 Some potential 17β-estradiol based anticancer drug molecules (**I-IX**) and 17β-estradiol.

[a]*Medicinal Chemistry Department,* [b]*Molecular Bioprospection Department and* [c]*Metabolic Structural Biology Departent, CSIR-Central Institute of Medicinal and Aromatic Plants, P.O. CIMAP, Kukrail Road, Lucknow 226015, India CSIR-Central Institute of Medicinal and Aromatic Plants, P.O. CIMAP, Kukrail Road, Lucknow 226015, India*

[d]*Division of Biochemistry, CSIR-Central Drug Research Institute, Sector-10, Jankipuram Extension, Lucknow 226 031, India, *To whom correspondence should be addressed: Tel: +915222718556, E-mail: atisky2001@yahoo.co.in,* *#CIMAP communication No.CIMAP/PUB/2015/02*

Since 17β-estradiol is a native ligand of estrogen receptor (ER), the possible hypothesis of using estrane in these molecules could be targeted delivery of therapeutics selectively to the target site. It is interesting to note that all these compounds possess estradiol as basic core which has been modified by incorporation of either by amino, amido, pentafluoroalkyl group or platinum complex at position 7, 15, 16 or 17 of steroid nucleus. These modification were made in such a way that modified groups could be accommodated spatially somewhere in the ring B and/or D region within LBD of ER. However, in this approach, incorporation of estrane nucleus sometimes creates secondary complications due its intrinsic estrogen agonistic action. Therefore, search for effective non-steroidal ligands for estrogen receptor such as tamoxifen and other non-steroidal antiestrogens warranted to address the issue.

Furthermore, quinazoline nucleus which is eventually present in lapatinib (**X**), erlotinib (**XI**), gefitinib (**XII**) and vandetanib (**XIII**) applied for the treatment of cancer, have been well explored for development of anticancer drugs Figure 2.[12-15] In our approach to device potential non-steroidal anticancer agents especially for estrogen receptor positive breast cancer treatment, we synthesized and evaluated 4-phenyl-5,6-dihydrobenzo[*h*]quinazolin derivatives for their anticancer potential. The designed molecules will have a quinazoline embedded tricyclic ring system analogus to rings A, B and C of estradiol and a phenyl ring bearing alkylamino or ester group flanked more towards ring D of estradiol core as presented in compounds **1-9**, Figures 1 and 2.

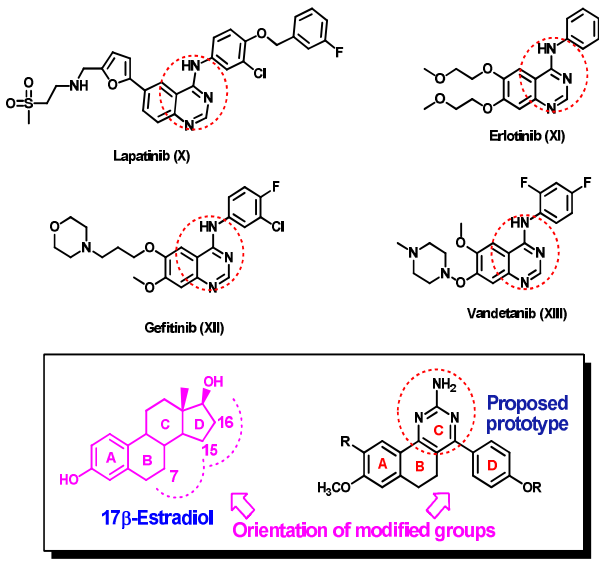

Fig. 2 Quinazoline fragment containing anticancer drugs, 17β-estradiol and proposed prototype.

Results and discussion

Chemistry

The synthesis of designed prototype was started with the preparation of different chalcones (**3**), an important intermediate for target compounds. Compound **3** was initially synthesized from the reaction of 1-tetralones (**1**) and substituted benzaldehydes (**2**) using BF_3-OEt_2 in dioxane in 72 h at room temperature under dry reaction conditions as reported by us.[16] Attempts were made to find out an alternate method for preparation of **3** which could yield **3** in short reaction time and do not require dry reaction conditions. For this purpose, we used N/10 HCl in aqueous medium at room temperature which offered simple reaction conditions, comparatively short reaction time (50h *vs* 72h) and formation of chalcone as sole product. However, yields of the product in this method were moderate. Further, attempts were made to improve the yields and the best conversion was observed at 50°C in 50h and used for chalcone synthesis (Scheme 1).

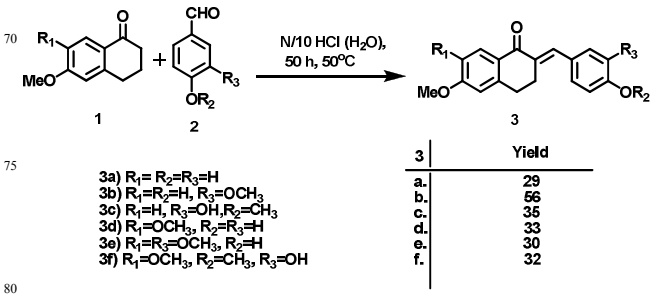

3	Yield
a.	29
b.	56
c.	35
d.	33
e.	30
f.	32

Scheme 1 Synthesis of chalcones (**3**).

Subsequently, targeted quinazoline analogs (**4**) were synthesized though the reaction of chalcone (**3**) with guanidine hydrochloride. For this purpose, we explored use of green solvents for synthesis of target compounds in short reaction time. In our attempts, we found choline chloride (ChCl) as an appropriate green, non toxic, environment benign solvent for synthesis of highly substituted 5,6-dihydro-8-methoxybenzo[*h*]quinazolin-amine (**4**) Scheme 2. The use of choline chloride (ChCl) containing eutectic solvents have been reported in various reactions in e.g. ChCl/urea supported conversion of aromatic boronic acid in phenol, ChCl/urea supported chemical fixation of carbon dioxide to cyclic carbonates, ChCl/glycine assisted biotransformations of ethyl valerate to butyl valerate, and bromination of substituted 1-aminoanthra-9,10-quinone, ChCl/L(-)-proline supported aldol reaction, Knoevenagel condensation in ChCl/amino acid, Diels-Alder cycloadditions and Fischer indole annulations in ChCl/$ZnCl_2$, ring opening of epoxides in ChCl/$SnCl_2$.[17-24]

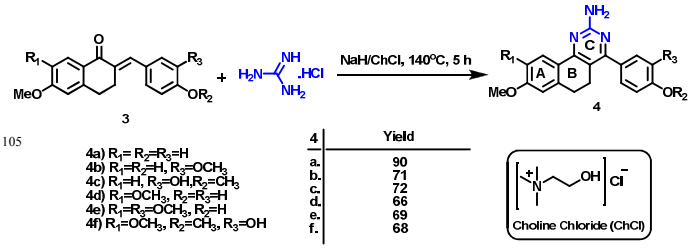

4	Yield
a.	90
b.	71
c.	72
d.	66
e.	69
f.	68

Scheme 2. Synthesis of benzo[*h*]quinazolin-2-amines (**4**).

Different reaction conditions were attempted in ChCl at different temperatures and molar ratio of reactants. The desired compounds were finally synthesized in good yields by the use of 1:1.2 molar ratios of reactants with NaH in ChCl at 140°C within 5h (Table 1). Interestingly, as reported by us, the use of conventional solvent such as dimethylformamide (DMF) under the reaction conditions takes longer reaction time *viz* 36h.[16]

Table1. Optimization of the reaction conditions

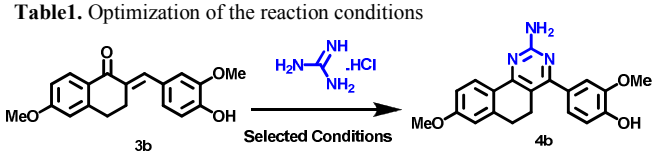

Entry	Base	Solvent	Temp (°C)	time (h)	purification	Yields
1	NaH (2 eq)*	DMF	120	36	required	53
2	NaH(2 eq)	THF	100	36	no reaction	0
3	NaH (2 eq)	THF-ChCl (1:2)	100	5	crystallization	85
4	KOH (2 eq)	H_2O-ChCl (1:2)	140	10	required	11
5	NaH (2 eq)	ChCl	140	5	crystallization	90

*Ref 16.

Furthermore, quinazoline (**4a**) was modified to alkylamine substituted quinazolines (**6**) though the reaction of substituted alkylamine hydrochlorides (**5**) with **4** in the presence of anhydrous K_2CO_3 in chloroform-acetone (1:1).[16] Similarly, alkylation of **4a** was done using bromo alkylesters the presence of potassium carbonate K_2CO_3 in chloroform-acetone (1:1) which yielded long chain ester substituted quinazoline (**8**) in 90-94% yields.[16]

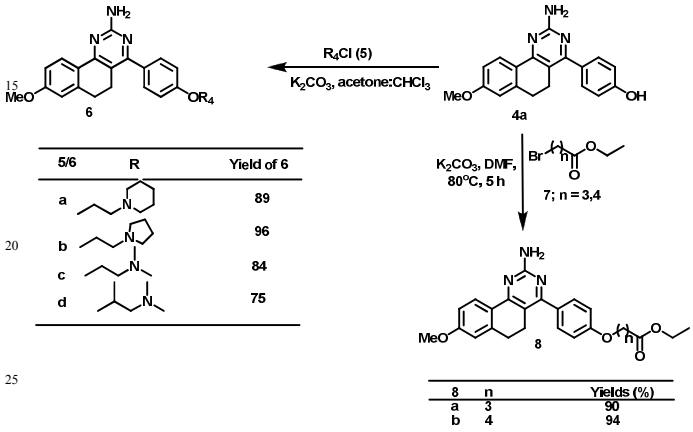

Scheme 3. Synthesis of benzo[*h*]quinazolin-2-amines derivatives (**6** and **8**).

The synthesized compounds were characterized by the use of different spectroscopic techniques viz NMR, IR, mass spectrometry.

Biology

The synthesized compounds were investigated for *in-vitro* growth inhibitory (anticancer) activity of cancer cells in a panel of cancer cell lines viz MCF-7 A549, FaDu and DU145 using SRB assay. Some promising molecules **(4a** and **6d)** were evaluated for their antitbulin activity using *in vitro* tubulin polymerization assay. Further, compound **6d** was evaluated for cell division cycle study using MCF-7 cells and its capability to induce apoptosis in cancer cells (MCF-7 cells) using PARP assay. The *in silico* docking experiments for **4a** and **6d** on estrogen receptor-α and tubulin protein were performed to verify the designing of these molecules. The results of these studies are elaborated in the following text.

In vitro growth inhibition of cancer cells

The compounds **4(a–f)**, **6(a–d)** and **8(a–b)** were explored for *in vitro* anticancer activity in various human carcinoma cell lines such as DLD1 (colorectal adenocarcinoma)**,** A549 (Lung carcinoma)**,** FaDu (hypopharyngeal carcinoma), MCF-7 (ER+ Breast adenocarcinoma), DU145 (prostate carcinoma) using sulphorhodamin B assay. Tamoxifen was used as positive control in this study. The anticancer activity of the tested compounds is described by half maximal inhibitory concentrations (IC_{50}) value in Table 2.

Among hydroxyl derivatives **4a-f,** compounds **4b** and **4c** which possessed methoxy and hydroxy groups in its ring D at positions 3 and 4 respectively presented anticancer activity in colon cancer cells at 1.87 and 6.79 µM concentrations whereas **4e** and **4f** which had two methoxy groups in ring A and methoxy and hydroxy groups in its ring D were devoid of anticancer activity. Compound **4d** which had two methoxy groups in ring A and a hydroxy group in its ring D showed significant anticancer activity in colon as well as prostate cancer cells at IC_{50} value 2.96 and 5.25 µM. Among others, compound **4a** which had a methoxy groups in ring A and a hydroxy group in its ring D presented potent anticancer activity in MCF-7, DLD-1, A549 and DU145 cancer cells at 5.89, 1.50, 1.86 and 1.50 µM concentrations respectively compared to tamoxifen, a positive control.

In order to improve the biological activity, compound **4a** was chosen for further modification. Interestingly, alkylation of **4a** with different tertiary aminoalkyl groups usually present in antiestrogens such as tamoxifen, yielded compounds which showed significant anticancer activity invariably in all cancer cell lines within the range of IC_{50} values 3.63-12.13 µM. Further, compound **8b** which had five carbon long chain ester group showed anticancer activity in MCF-7, DLD1, and A549 cells at 8.03, 15.10 and 12.99 µM concentrations respectively whereas another ester analog **8a** was devoid of any activity upto **20** µM concentration.

Tubulin Polymerization Inhibition

Microtubule/tubulin dynamics interrupting molecules bind to the tubulin protein which perturb mitosis and arrest growth of cells during interphase.[25] Having growth inhibitory activity data in our hands, we next wished to evaluate whether or not these molecules could inhibit the growth of cancer cells through inhibition of tubulin polymerization. For this purpose, compounds **4a** and **6d** were evaluated for tubulin polymerization inhibitory activity using tubulin protein in *in-vitro* model. In this experiment, podophyllotoxin and nocadazole, standard tubulin polymerization inhibitors, were used as positive control and DMSO as negative control. Compounds **4a** and **6d** effectively inhibited tubulin polymerization at IC_{50} value 2.92 and 5.97 µM respectively. Compound **6d** presented antitubulin activity very close to the podophyllotoxin.

Table 2 *In vitro* anticancer activity of compounds **4** (**a-f**), **6(a-d)** and **8** (**a-b**) using SRB assay **(IC_{50} in μM)**[#,*]

Compounds	Carcinoma cell lines (IC_{50} in μM, mean±SE)				
	MCF-7	DLD1	A549	DU145	FaDu
4a	5.89±1.22	<1.50	1.86±0.18	<1.50	[a]
4b	>20	<1.87	>20	[c]	[a]
4c	>20	6.79±1.14	>20	>20	[a]
4d	>20	2.96	>20	5.25	[a]
4e	>20	>20	>20	>20	[a]
4f	>20	>20	>20	>20	[a]
6a	7.09±0.66	3.90±0.82	7.97±0.19	7.82±1.17	7.59±1.01
6b	12.13±0.54	6.64±1.22	11.36±0.54	10.41±1.48	9.92±0.94
6c	7.84±0.91	4.22±0.94	8.05±0.18	7.76±1.41	7.51±1.28
6d	6.38±0.37	3.63±0.71	7.35±0.11	6.96±1.27	6.44±0.55
8a	>20	>20	>20	>20	>20
8b	8.03±0.62	15.10 [b]	12.99±0.72	>20	>20
Tamoxifen	8.74±1.17	14.65	10.37±0.84	12.14±0.62	[a]

#values are represented as mean IC_{50} value±SE of three independent experiments. The concentration of compounds used for IC_{50} determination was 5 serial dilutions (2 fold) of the 20μM starting concentration .The ‡incubation period of drug treated cells was 48h. *Cell lines used: **DLD1** (colorectal adenocarcinoma)**, A549** (Lung carcinoma)**, FaDu** (hypopharyngeal carcinoma), **MCF-7** (ER+ Breast adenocarcinoma), **DU145** (prostate carcinoma), [a] = not done.

Table 3 Tubulin polymerization inhibition of **4a** and **6d** using tubulin polymerization assay (half maximal inhibitory concentrations, IC_{50} in μM)[#]

S.No.	Compound	IC 50 (μM)
1	**4a**	5.97±0.7
2	**6d**	2.92±0.16
3	**Podophyllotoxin (PDT)**	2.27±0.6
4	**Nocadazole**	2.06±0.07

#values are represented as mean IC_{50} value±SE of three independent experiments

Cell division cycle study of 6d

Further, compound **6d** was selected for Cell division cycle study using estrogen receptor (ER) positive human breast cancer cell line (MCF-7). After 24 and 48 hrs incubation with **6d** at 7 μM concentration (near IC_{50} value), substantial accumulation of cells population at sub-G_0 (apoptotic) and G_0/G_1 phase compared to the vehicle treated controls was observed in a time dependent manner (Figure 3a-b). This was associated with concomitant decrease in cells at S phase while there was no obvious change in G_2/M population.

Cell apoptosis study

Following anticancer, tubulin polymerization inhibitory activity and cell cycle study of **6d**, we further investigated ability of **6d** to trigger apoptosis in MCF-7 cells by Western blot assay after probing with anti-PARP antibody. Poly (ADP-ribose) polymerase (PARP) is a protein which is involved in a number of cellular processes including DNA repair and programmed cell death through the production of PAR, which stimulates mitochondria to release apoptosis-inducing factor (AIF).[26] In the present study, we monitored cleavage of Poly (ADP-ribose) polymerase (PARP) which is considered as a marker of apoptosis. Consistent with flowcytometry data, Western blot analyses of MCF-7 cell lysates revealed proteolysis of PARP in **6d** treated cells confirming induction of apoptosis (Figure 4). In this experiment, doxorubicin (doxo), a potent anticancer drug was used as positive control.

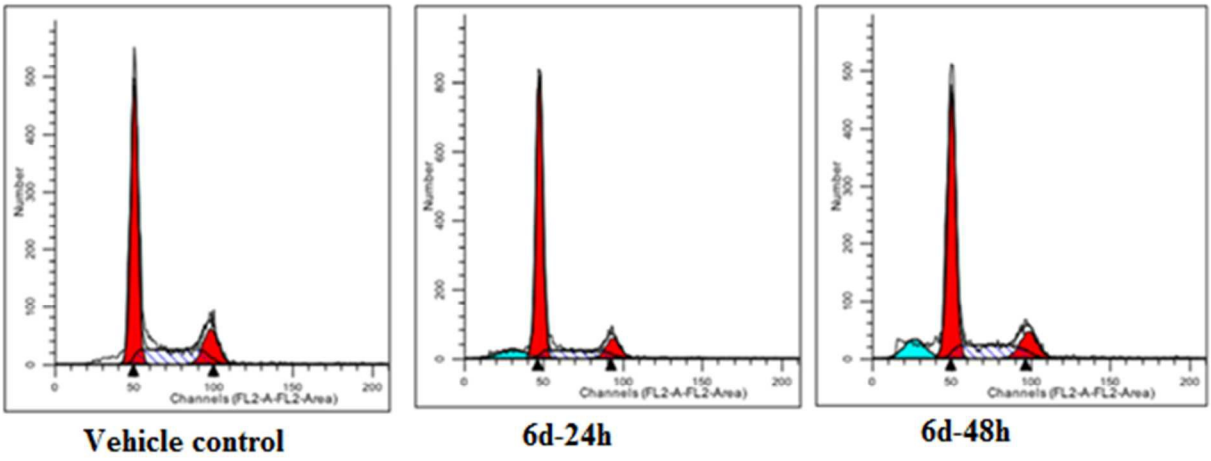

Fig. 3a

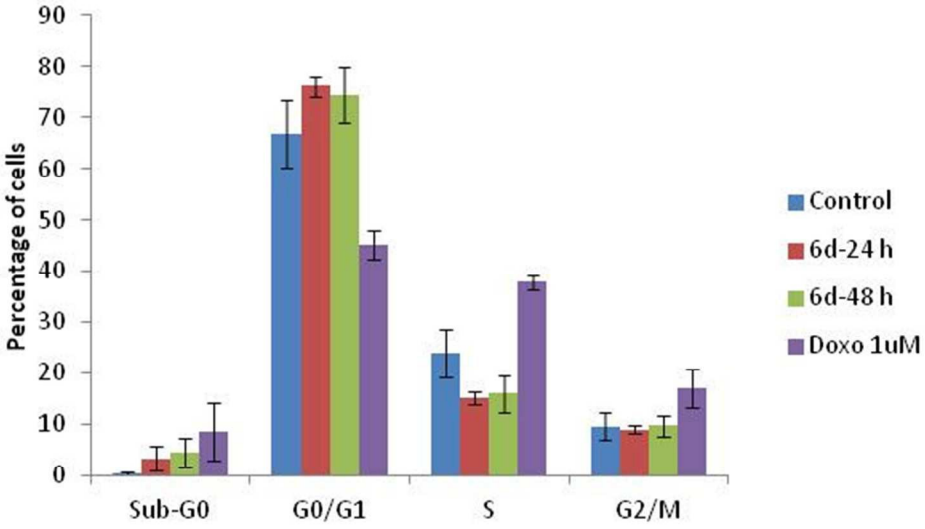

Fig. 3b

Fig. 3 Effect of **6d** on cell division cycle (a) MCF-7 cells were treated with **6d** at IC_{50} concentrations for 24 h and 48 h, stained with propidium iodide(PI) and were subjected to flow cytometry. (b) Histogram showing average population cells in various phases (G1, G2, S) of cell cycle (mean ± S.E. of three independent assays, each performed in duplicate). $^{\#}P$ <0.05, $*P$ <0.001 compared with vehicle treated controls.

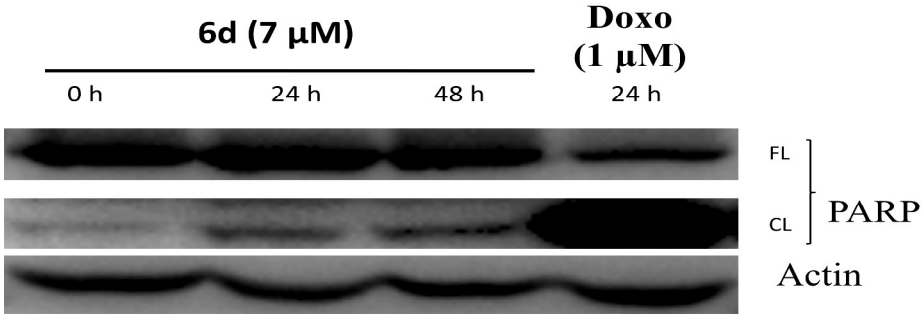

Fig. 4 6d induces apoptosis in MCF-7 cells. Lysates from treated and untreated cells were subjected to immunoblotting after probing with anti-PARP antibody. Marked cleavage of PARP was observed in **6d** treated cells in time dependent manner.

Docking Study

To investigate the mechanism of action of studied molecules, a molecular docking study was performed for **4a** and **6d** against targets ER-α and tubulin using Autodock MGL tool v1.5.6. The docking study with estrogen receptor-α (ER-α) revealed that compounds **4a** and **6d** exhibit promising binding affinity within the tamoxifen binding site with docking binding energy -7.12 kcal mol^{-1} (Ki value 6.01 µM) and -5.55 kcal mol^{-1} (Ki value 84.85 µM) respectively. The identified key residues for ligand-receptor interaction are ARG 394, THR 347 and GLY 420. The –NH2 group of amino acid arginine interact with oxygen atom of hydroxyl group of molecules **4a** and **6d** with bond distance 2.79 and 2.80 Å respectively. The compound **4a** is making two additional H-bonds with amino acid residues THR 347 and GLY 420 having bond distance 2.07 and 1.7 Å. The results are summarized in table 4 and 5.

Similarly, the interaction study of molecules with tubulin protein indicate that control Podophyllotoxin, **4a** and **6d** showed good binding affinity within the colchicine binding site of tubulin protein. 4a exhibit highest docking binding energy of -5.59 kcal mol^{-1} (Ki value 79.52 µM) and making two H-bonds with amino acid residues ALA 317 and LYS 352 having bond distance 2.198 and 2.229 Å. Whereas compound **6d** showed moderate docking binding energy of -5.06 kcal mol^{-1} (Ki value 194.67 µM).

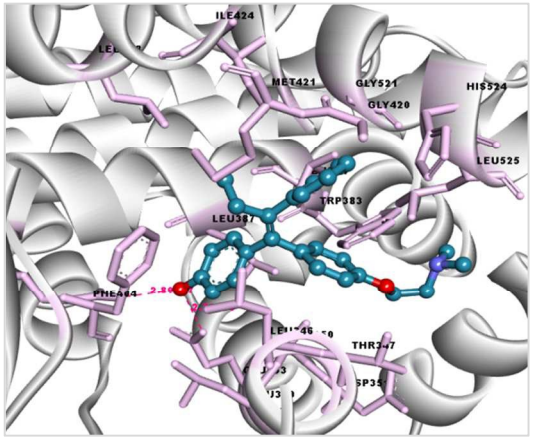

Fig.5a

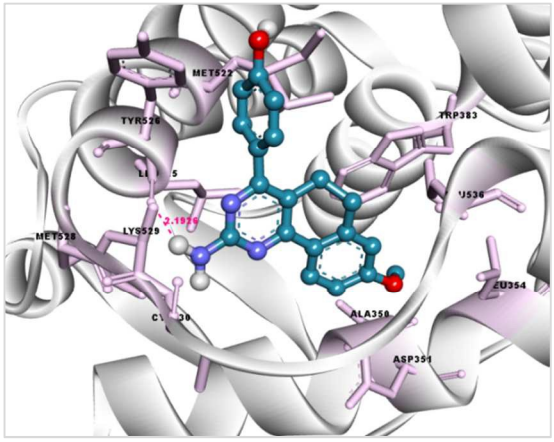

Fig.5b

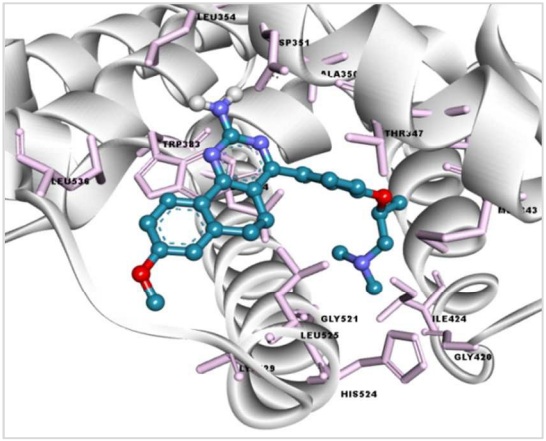

Fig.5c

Fig. 5. **(a)** Docking pose of tamoxifen within LBD of Estrogen Receptor-α, (**b**) Docking pose of **4a** within LBD of Estrogen Receptor-α (**c**) Docking pose of **6d** within LBD of Estrogen Receptor-α. The residues are highlighted with pink stick, ligand is represented with blue ball and stick form and H-bonding is represented with dashed lines.

Table 4 Docking interactions of **tamoxifen, 4a and 6d** within ligand binding pocket of estrogen receptor-α (ERα).

Compounds	Binding energy (kcal mol^{-1})	Ki value (inhibitory constant)	Binding pocket residues within 4Å region	Interacting residues and H-bond length (Å)	Number rotatable bonds
Tamoxifen	-8.89	304.35 nM	MET343, LEU346, THR347, ALA350, ASP351, GLU353, TRP383, LEU384, LEU387, MET388, LEU391, ARG394, PHE404, GLU419, GLY420, MET421, ILE424, LEU428, GLY521, HIS524, LEU525	ARG394 :NH2-Tamoxifen: O4 (2.8) & Tamoxifen:O4-GLU353:OE2 (2.4)	8
4a	-7.12	6.01 uM	MET343, LEU346, THR347, LEU349, ALA350, GLU353, LEU384, LEU387, ARG394, GLU419, GLY420, MET 421, ILE424GLY521, HIS 524, LEU525	ARG394:NH2-4a: O (2.79572), 4a: H-THR347:OG1 (2.0738) & 4a: H-GLY420: O (1.73547)	2
6d	-5.55	84.85 uM	MET343, LEU346, THR347, ALA350, ASP351, GLU353, TRP383, LEU384, LEU387, MET388, LEU391, ARG394, ILE424, GLY521, LEU525, MET528	ARG394:NH2-6d: O (2.80547)	6

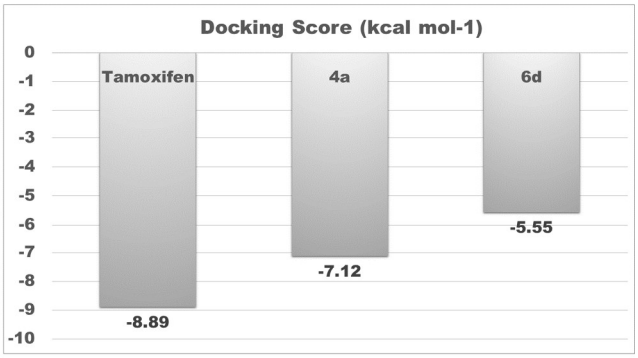

Fig. 6 Binding affinity of **tamoxifen**, **4a** and **6d** with estrogen receptor-α (ERα).

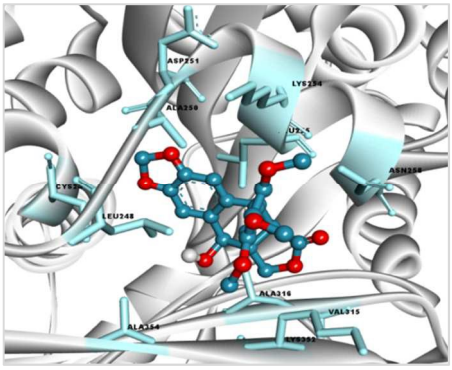

Fig.7a

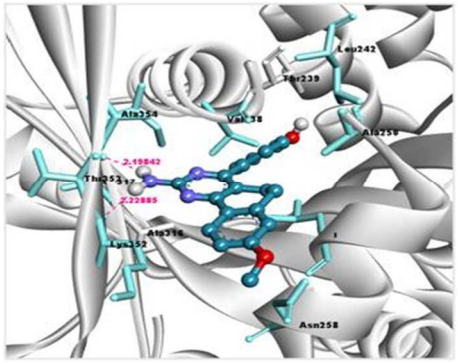

Fig.7b

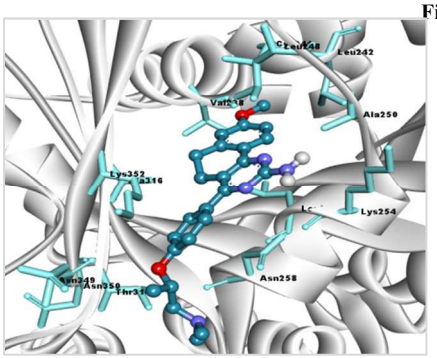

Fig.7c

Fig. 7 (**a**) Docking pose of **podophyllotoxin** within the binding site of tubulin, (**b**) Docking pose of **4a** within the binding site of tubulin, (**c**) Docking pose of **6d** within the binding site of tubulin. Binding pocket residues are highlighted with cyan color stick form, ligand is represented with blue ball and stick form and H-bonding is represented with dashed lines.

Table 5 Docking interactions of podophyllotoxin, **4a** and **6d** with binding site residues of β-tubulin and comparison of binding affinity of in terms of docking energy.

Compounds	Binding energy (kcal mol^{-1})	Ki value (inhibitory constant)	Binding pocket residues within 4Å region	Interacting residues and H-bond length (Å)	Number rotatable bonds
Podophyllotoxin	-5.16	165.71 uM	CYS241, LEU248, ALA250, ASP251, LYS254, LEU255, ASN258, VAL315, ALA316, LYS352, ALA354	-	5
4a	-5.59	79.52 uM	VAL238, THR239, CYS241, LEU242, LEU248, ALA250, LEU255, ASN258, ALA316, ALA317, ILE318, LYS352, THR353, ALA354	4a: H-ALA317:O (2.19842) & 4a:H-LYS352:O (2.22885)	2
6d	-5.06	194.67 uM	VAL238, CYS241, LEU242, LEU248, ALA250, LYS254, LEU255, ASN258, MET259, THR314, ALA316, ILE347, PRO348, ASN349, ASN350, LYS352	-	6

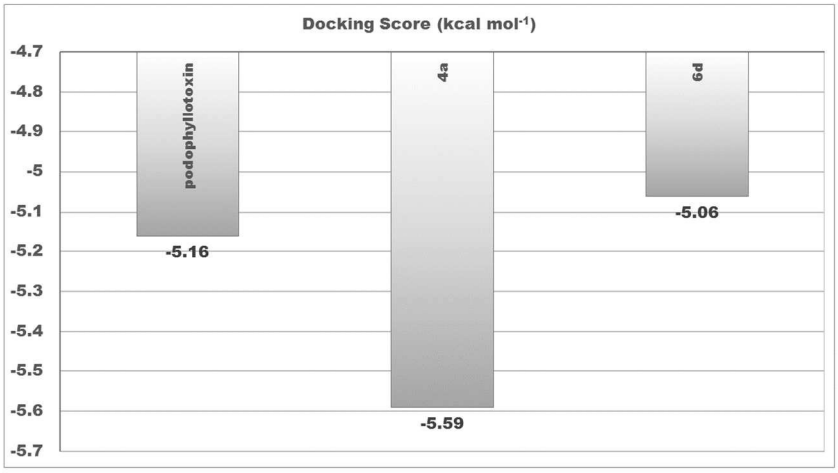

Fig. 8 Binding affinity of **tamoxifen**, **4a** and **6d** with binding site residues of β-tubulin.

Conclusion

In conclusions, we have established a greener approach for synthesis of substituted benzo[*h*]quinazoline analogs from chalcones and guanidine in good yields. The synthesized compounds presented significant anticancer activity in a panel of cancer cell lines. The cell apoptosis and tubulin polymerization inhibitory activities of promising molecule **6d**, revealed that the anticancer activity of compound is due to apoptosis of cancer cell which is very likely due to its tubulin polymerization inhibitory activity. The *in-silico* docking experiments of **4a** and **6d** showed that these molecules have ability to interact with estrogen receptor-α and colchicine binding site of tubulin protein. The biological activity and *in-silico* study results indicate that structural arrangement of **6d** allows it to interact with β-tubulin for its anticancer activity in general and has estrogen receptor mediated activity in ER positive cancer cells (MCF-7 cells) in particular. Further, structural modifications of these 4-phenyl-5,6-dihydrobenzo[*h*]quinazolins may lead to effective and ER selective anticancer lead molecules.

Experimental Section

General

The reagents and the solvents used in this study were of analytical grade and used without further purification. All the reactions were monitored on Merck aluminium thin layer chromatography (TLC, UV_{254nm}) plates. Column chromatography was carried out on silica gel (60-120 mesh). The melting points were determined on Buchi melting point M560 apparatus in open capillaries and are uncorrected. Commercial reagents were used without purification. ^{1}H and ^{13}C NMR spectra were recorded on a Bruker WM-300 (300 MHz) using $CDCl_3$ and DMSO-d_6 as the solvent. Chemical shift are reported in parts per million shift (δ-value) based on the

middle peak of the solvent ($CDCl_3$/DMSO-d_6) (δ 75.00 ppm for ^{13}C NMR) as the internal standard. Signal patterns are indicated as s, singlet; bs, broad singlet; d, doublet; dd, double doublet; t, triplet; m, multiplet; brm, broad multiplet. Coupling constants (*J*) are given in Hertz. Infrared (IR) spectra were recorded on a Perkin-Elmer AX-1 spectrophotometer in KBr disc and reported in wave number (cm^{-1}). ESI mass spectra were recorded on Shimadzu LC-MS after dissolving the compounds in acetonitrile and methanol.

General procedure for the synthesis of compounds (3a-f)

(E)-2-(4-hydroxybenzylidene)-6-methoxy-3,4-dihydronaphthalen-1(2H)-one (3a)

In a round bottomed flask, substituted tetralone (**1,** R_1= H, 3.52 g, 2.00 mmol) was stirred in N/10 ml aqueous HCl (10 mL) and substituted benzaldehyde (**2,** R_2 = H, R_3 = H, 2.44 g, 2.00 mmol) was added in the reaction mixture. The reaction mixture was allowed to stir at 50 ^oC for 50 h. The progress of reaction was monitored using TLC. After completion of reaction, the reaction content was filtered and crude material was subjected to column chromatography on silica gel using ethyl acetate-hexane as eluent get desired compound (**3a**) as yellow solid.

Yellow solid, R_f: 0.3 (30% EtOAc in hexane); mp 172-173^oC; IR (KBr, ν_{max}/cm^{-1}): 3357 (NH_2), 3489 (OH); ^1H NMR (acetone-d_6, 300 MHz, δ ppm): 2.92 (t, 2H, *J* = 6.0 Hz, CH_2), 3.11 (t, 2H, *J* = 6.0 Hz, CH_2), 3.88 (s, 3H, OCH_3), 6.90 (m, 4H, ArH), 7.39 (d, 2H, *J* = 8.4 Hz, ArH), 7.68 (s, 1H, CH), 7.97 (d, 1H, *J* = 8.4 Hz, ArH), 9.35 (s, 1H, OH); ^{13}C NMR (acetone-d_6, 75 MHz, δ ppm): 27.60, 29.30, 55.58, 112.66, 113.87, 116.05 (2xC), 127.50, 127.64, 130.49, 132.36 (2xC), 133.54, 136.02, 146.27, 159.04, 164.03, 185.96; ESIMS ($C_{18}H_{16}O_3$): m/z : 281 $[M+H]^+$.

(E)-2-(4-hydroxy-3-methoxybenzylidene)-6-methoxy-3,4-dihydronaphthalen-1(2H)-one (3b)

Yellow solid, R_f: 0.4 ($CHCl_3$); mp 129-130^oC; ^1H NMR ($CDCl_3$, 300 MHz, δ ppm): 2.90 (t, 2H, *J* = 6.3 Hz, CH_2), 3.12 (t, 2H, *J* = 6.3 Hz, CH_2), 3.85 (s, 3H, OCH_3), 3.90 (s, 3H, OCH_3), 5.91 (s, 1H, OH), 6.68 (s, 1H, ArH), 6.69 (d, 1H, *J* = 2.4 Hz, ArH), 6.84-7.03 (m, 3H, ArH), 7.77 (s, 1H, CH), 8.10 (d, 1H, *J* = 8.7 Hz, ArH); ^{13}C NMR ($CDCl_3$, 75 MHz, δ ppm): 27.71, 29.62, 55.83, 56.39, 112.66, 113.19, 113.64, 114.84, 124.08, 127.59, 128.76, 131.09, 134.15, 136.76, 145.95, 146.69, 146.81, 163.90, 187.14; ESIMS ($C_{19}H_{18}O_4$): m/z = 311 $[M+H]^+$.

(E)-2-(3-hydroxy-4-methoxybenzylidene)-6-methoxy-3,4-dihydronaphthalen-1(2H)-one (3c)

Yellow solid, R_f: 0.26 (22% EtOAc in hexane); mp 173-174^oC; ^1H NMR (DMSO-D_6, 300 MHz, δ ppm): 2.87 (t, 2H, *J* = 6.3 Hz, CH_2), 3.01 (t, 2H, *J* = 6.3 Hz, CH_2), 3.77 (s, 3H, OCH_3), 3.80 (s, 3H, OCH_3), 6.85-6.94 (m, 5H, ArH), 7.87 (s, 1H, CH), 9.18 (s, 1H, OH); ^{13}C NMR (DMSO-D_6, 75 MHz, δ ppm): 27.58, 29.10, 56.36, 56.49, 112.94, 113.12, 114.44, 117.69, 123.10, 127.34, 128.99, 130.67, 134.21, 136.23, 146.64, 147.18, 149.31, 164.01, 186.30; ESIMS ($C_{19}H_{18}O_4$): m/z = 349 $[M+K]^+$.

(E)-2-(4-hydroxybenzylidene)-6,7-dimethoxy-3,4-dihydronaphthalen-1(2H)-one (3d)

Yellow solid, R_f: 0.53 (50% EtOAc in hexane); mp 247-248^oC; UV(CH_3CN, λ_{max}/nm (ε/dm^3 mol^{-1} cm^{-1}): 238 nm (300), 355 nm (400); ^1H NMR ($CDCl_3$+DMSO-D_6, 300 MHz, δ ppm): 2.90 (t, 2H, *J* = 6.0 Hz, CH_2), 3.11 (t, 2H, *J* = 6.0 Hz, CH_2), 3.89 (s, 3H, OCH_3), 3.92 (s, 3H, OCH_3), 6.74 (s, 1H, ArH), 6.87 (d, 2H, *J* = 8.4 Hz, ArH), 7.32 (d, 2H, *J* = 8.4 Hz, ArH), 7.53 (s, 1H, CH), 7.67 (s, 1H, ArH), 9.50 (s, 1H, OH); ^{13}C NMR ($CDCl_3$+DMSO-D_6, 75 MHz, δ ppm): 32.56, 33.49, 61.12, 61.22, 114.79, 115.47, 120.87 (2xC), 131.77, 131.99, 136.96 (2xC), 137.77, 141.33, 143.29, 153.29, 158.58, 163.47, 191.41; ESIMS ($C_{19}H_{18}O_4$): m/z = 349 $[M+K]^+$.

(E)-2-(4-hydroxy-3-methoxybenzylidene)-6,7-dimethoxy-3,4-dihydronaphthalen-1(2H)-one (3e)

Yellow solid, R_f: 0.33 ($CHCl_3$); mp 157-158^oC; ^1H NMR ($CDCl_3$, 300 MHz, δ ppm): 2.87 (t, 2H, *J* = 6.0 Hz, CH_2), 3.11 (t, 2H, *J* = 6.0 Hz, CH_2), 3.89 (s, 3H, OCH_3), 3.92 (s, 6H, 2xOCH_3), 5.92 (s, 1H, OH), 6.65 (s, 1H, ArH), 6.92-7.02 (m, 3H, ArH), 7.60 (s, 1H, CH), 7.75 (s, 1H, ArH); ^{13}C NMR ($CDCl_3$, 75 MHz, δ ppm): 27.92, 28.95, 56.39, 56.47 (2xC), 110.14, 110.29, 113.20, 114.85, 124.03, 127.13, 128.76, 133.98, 136.73, 138.42, 146.67, 146.83, 148.67, 153.88, 187.12; ESIMS ($C_{20}H_{20}O_5$) : m/z = 341 $[M+H]^+$.

(E)-2-(3-hydroxy-4-methoxybenzylidene)-6,7-dimethoxy-3,4-dihydronaphthalen-1(2H)-one (3f)

Yellow solid, R_f: 0.32 ($CHCl_3$); mp 169-170^oC; ^1H NMR ($CDCl_3$, 300 MHz, δ ppm): 2.86 (t, 2H, *J* = 6.3 Hz, CH_2), 3.11 (t, 2H, *J* = 6.3 Hz, CH_2), 3.90 (s, 3H, OCH_3), 3.92 (s, 6H, 2xOCH_3), 5.75 (s, 1H, OH), 6.65 (s, 1H, ArH), 6.87 (d, 1H, *J* = 8.1 Hz, ArH), 6.96 (d, 1H, *J* = 8.1 Hz, ArH), 7.05 (d, 1H, *J* = 1.5 Hz, ArH), 7.60 (s, 1H, CH), 7.72 (s, 1H, ArH); ^{13}C NMR ($CDCl_3$, 75 MHz, δ ppm): 27.86, 28.95, 56.39, 56.48, 110.11, 110.29, 110.89, 116.14, 116.38, 123.43, 127.12, 129.88, 134.38, 136.22, 136.38, 138.52, 145.76, 147.32, 148.64, 153.86, 187.17; ESIMS ($C_{20}H_{20}O_5$) : m/z = 339 $[M-H]^+$.

General procedure for the synthesis of compounds (4a-f)

8-Methoxy-4-phenyl-5,6-dihydrobenzo[h]quinazolin-2-amine (4a)

In a 100 mL round bottom flask, NaH (50 mg, 2.00 mmol) and guanidine hydrochloride (1.43 g, 1.50 mmol) in choline chloride (ChCl) (10 mL) was stirred on ice bath at 0^oC for 10 minutes. Afterwards, **3a** (2.80 g, 1.00 mmol)) dissolved in choline chloride (ChCl, 2.5 mL) was added to the reaction mixture and reaction mixture was allowed to stirred at 140°C for 5 h. The progress of reaction was monitored by thin layer chromatography. After the completion of reaction, the mixture was diluted with water and extracted with ethyl acetate. The organic phase was separated, dried over anhydrous sodium sulphate and concentrated to give crude material which on column chromatography on basic alumina using methanol in chloroform as eluent gave desired compound **4a.**

Off-white solid, R_f: 0.17 (10% methanol in chloroform); mp 263-265^oC; IR (KBr, ν_{max}/cm^{-1}): 3357 (NH_2), 3489 (OH); ^1H NMR (DMSO-D_6, 300 MHz, δ ppm): 2.74 (bs, 2xCH_2), 3.80 (s, 3H, OCH_3), 5.74 (s, 1H, OH), 6.31 (s, 2H, NH_2), 6.83-6.92 (m, 4H, ArH), 7.42 (d, 2H, *J* = 8.4 Hz, ArH), 8.09 (d, 1H, *J* = 8.4 Hz, ArH); ^{13}C NMR (DMSO-D_6, 75 MHz, δ ppm): 24.71, 28.94, 56.09, 113.38, 113.50, 113.77, 115.52 (2xC), 126.86, 127.63,

129.97, 131.14 (2xC), 142.19, 158.86, 160.50, 161.78, 162.81, 165.07; ESIMS ($C_{19}H_{17}N_3O_2$): m/z = 320.4 $[M+H]^+$.

4-(2-amino-8-methoxy-5,6-dihydrobenzo[h]quinazolin-4-yl)-2-methoxyphenol (4b)

Off-white solid, R_f: 0.57 (10% methanol in chloroform); mp 271-272 °C; UV (CH_3CN, λ_{max}/nm (ε/dm^3 mol^{-1} cm^{-1}): 203 nm (280), 224 nm (150), 280 nm (90), 348 nm (110); ^{1}H NMR (DMSO-D_6, 300 MHz, δ ppm): 2.69-2.76 (m, 2xCH_2), 3.73 (s, 3H, OCH_3), 3.76 (s, 3H, OCH_3), 6.10 (bs, 2H, NH_2), 6.73 (d, 1H, *J* = 8.1 Hz, ArH), 6.80 (d, 1H, *J* = 2.1 Hz, ArH), 6.85 (d, 1H, *J* = 2.4 Hz, ArH), 6.88 (m, 1H, ArH), 7.04 (s, 1H, ArH), 8.03 (d, 1H, *J* = 8.7 Hz, ArH); ^{13}C NMR (DMSO-D_6, 75 MHz, δ ppm): 24.74, 28.91, 56.10, 56.57, 113.49, 113.78, 114.03, 115.69, 122.69, 126.71, 127.67, 142.21, 148.00, 148.40, 161.82, 162.63; ESIMS ($C_{20}H_{19}N_3O_3$): m/z = 350 $[M+H]^+$.

4-(2-amino-8-methoxy-5,6-dihydrobenzo[h]quinazolin-4-yl)-2-methoxyphenol (4c)

Off-white solid, R_f: 0.56 (10% methanol in chloroform); mp 223-224°C; UV (CH_3CN, λ_{max}/nm (ε/dm^3 mol^{-1} cm^{-1}): 204 nm (760), 226 nm (450), 279 nm (250), 347 nm (350); ^{1}H NMR (DMSO-D_6, 300 MHz, δ ppm): 2.76 (bs, 4H, 2xCH_2), 3.81 (s, 6H, 2xOCH_3), 6.31 (s, 2H, NH_2), 6.86-7.04 (m, 5H, ArH), 8.10 (d, 1H, *J* = 8.4 Hz, ArH), 9.15 (s, 1H, OH); ^{13}C NMR (DMSO-D_6, 75 MHz, δ ppm): 24.70, 28.99, 56.20, 56.57, 113.52, 113.75, 117.26, 117.37, 120.96, 127.01, 127.75, 132.57, 142.20, 146.91, 146.94, 149.32, 161.00, 162.11, 162.79, 165.23; ESIMS ($C_{20}H_{19}N_3O_3$): m/z = 350 $[M+H]^+$.

4-(2-amino-8-methoxy-5,6-dihydrobenzo[h]quinazolin-4-yl)-2-methoxyphenol (4d)

Off-white solid, R_f: 0.11 (2% methanol in chloroform); mp 248-249°C; UV (CH_3CN, λ_{max}/nm (ε/dm^3 mol^{-1} cm^{-1}): 204 nm (250), 225 nm (160), 279 nm (110), 354 nm (10 0); ^{1}H NMR (DMSO-d_6, 300 MHz, δ ppm): 2.75 (bs, 2xCH_2), 3.81 (s, 6H, 2xOCH_3), 6.27 (s, 2H, NH_2), 6.83 (s, 1H, ArH), 6.87 (d, 2H, *J* = 6.9 Hz, ArH), 7.42 (d, 2H, *J* = 8.4 Hz, ArH), 7.70 (s, 1H, ArH), 8.25 (s, 1H, OH); ^{13}C NMR (DMSO-d_6, 75 MHz, δ ppm): 24.87, 28.11, 56.42 (2xC), 109.07, 111.91, 113.88, 115.54 (2xC), 126.00, 126.26, 131.12 (2xC), 133.74, 148.39, 151.58, 158.80, 160.55, 162.70, 165.04; ESIMS ($C_{20}H_{19}N_3O_3$): m/z = 350 $[M+H]^+$.

4-(2-amino-8-methoxy-5,6-dihydrobenzo[h]quinazolin-4-yl)-2-methoxyphenol (4e)

Off-white solid, R_f: 0.34 (EtOAc); mp 271-272°C; UV(CH_3CN, λ_{max}/nm (ε/dm^3 mol^{-1} cm^{-1}): 209 nm (400), 281 nm (100), 313 nm (60), 357 nm (160); ^{1}H NMR (DMSO-d_6, 300 MHz, δ ppm): 2.70 (bs, 2H, CH_2), 2.83 (bs, 2H, CH_2), 3.75 (s, 3H, OCH_3), 3.81 (s, 3H, 2xOCH_3), 6.18 (s, 2H, NH_2), 6.71 (d, 1H, *J* = 8.1 Hz, ArH), 6.88 (s, 1H, ArH), 6.94 (d, 1H, *J* = 8.1 Hz), 7.08 (s, 1H, ArH), 7.70 (s, 1H, OH), ^{13}C NMR (DMSO-d_6, 75 MHz, δ ppm): 25.33, 28.30, 56.44, 56.50 (2xC), 109.14, 111.89, 113.61, 114.30, 116.66, 123.72, 126.63, 133.55, 142.00, 148.36, 149.40, 151.39, 154.00, 160.19, 162.59, 165.65; ESIMS ($C_{21}H_{21}N_3O_4$): m/z = 380.4 $[M+H]^+$.

4-(2-amino-8-methoxy-5,6-dihydrobenzo[h]quinazolin-4-yl)-2-methoxyphenol (4f)

Off-white solid, R_f: 0.66 (EtOAc); mp 223-224°C; UV(CH_3CN, λ_{max}/nm (ε/dm^3 mol^{-1} cm^{-1}): 208 nm (230), 282 nm (70), 313 nm (60), 357 nm (90); ^{1}H NMR (DMSO-d_6, 300 MHz, δ ppm): 2.62 (t, 2H, *J* = 4.5 Hz, CH_2), 2.70 (t, 2H, *J* = 4.5 Hz, CH_2), 3.75 (s, 3H, OCH_3), 3.80 (s, 3H, OCH_3), 3.81 (s, 3H, OCH_3), 6.25 (s, 2H, NH_2), 6.74 (d, 1H, *J* = 1.8 Hz, ArH), 6.84 (s, 1H, ArH), 6.86 (s, 1H, ArH), 6.96 (d, 1H, *J* = 1.2 Hz, ArH), 7.70 (s, 1H, ArH); 7.70 (s, 1H, OH); ^{13}C NMR (DMSO-d_6, 75 MHz, δ ppm): 24.92, 28.13, 56.40, 56.47 (2xC), 109.05, 111.88, 112.23, 113.94, 117.52, 118.39, 126.31, 132.04, 133.74, 148.36, 149.88, 150.06, 151.52, 160.37, 162.65, 165.66; ESIMS ($C_{21}H_{21}N_3O_4$): m/z = 380 $[M+H]^+$.

General procedure for the synthesis of compounds (6a-d)

4-(4-(2-(piperidin-1-yl)ethoxy)phenyl)-5,6-dihydro-8-methoxybenzo[h] quinazolin-2-amine (6a)

In a round bottom Flask, 4-(2-amino-5,6-dihydro-8-methoxybenzo[h]quinazolin-4-yl)phenol (**4a,** 320 mg, 1.00 mmol) was stirred in the mixture of acetone (40 mL) and chloroform (25 mL) at 80°C. After stirring for ten minutes, anhydrous K_2CO_3 (210 mg, 1.50 mmol) and 2-piperidinylethylchloride hydrochloride **5** (2.40 mg, 1.30 mmol) was added in reaction mixture. The progress of reaction was monitored by thin layer chromatography. After the completion of the reaction, solvent was evaporated and residue was diluted with chloroform and extracted with water. The organic phase was separated, evaporated and dried. The crude was purified by column chromatography with a mixture of chloroform-hexane (10%) to give the desired product **6a**.

Off-white solid; R_f: 0.23 (10% methanol in chloroform); mp 152-155°C; IR (KBr, ν_{max}/cm^{-1}): 3396 (NH_2); ^{1}H NMR ($CDCl_3$, 300 MHz, δ ppm): 1.26 (bs, 2H, CH_2), 1.46 (bs, 4H, 2xCH_2), 2.54 (bs, 4H, 2xNCH_2), 2.77-2.86 (bs, 6H, NCH_2 & 2xCH_2), 3.85 (s, 3H, OCH_3), 4.17 (t, 2H, OCH_2), 5.00 (s, 2H, NH_2), 6.73 (d, 1H, *J* = 2.1 Hz, ArH), 6.86 (d, 1H, *J* = 2.4 Hz, ArH), 6.89 (d, 2H, *J* = 2.1 Hz, ArH), 7.50 (d, 2H, *J* = 8.7 Hz, ArH), 8.20 (d, 1H, *J* = 8.7 Hz, ArH); ^{13}C NMR ($CDCl_3$, 75 MHz, δ ppm): 24.52, 24.73, 26.24 (2xC), 29.16, 55.43 (2xC), 55.72, 58.20, 66.41, 112.95, 113.24, 114.72 (2xC), 115.43, 126.67, 127.83, 130.54 (2xC), 131.41, 141.92, 159.79, 161.36, 161.94, 161.98, 165.04; ESIMS ($C_{26}H_{30}N_4O_2$): m/z = 431.5 $[M+H]^+$.

4-(4-(2-(pyrrolidin-1-yl)ethoxy)phenyl)-5,6-dihydro-8-methoxybenzo[h]quinazolin-2-amine (6b)

Off-white solid; R_f: 0.23 (10% methanol in chloroform); mp 118-122°C; IR (KBr, ν_{max}/cm^{-1}): 3398 (NH_2); ^{1}H NMR (DMSO-D_6, 300 MHz, δ ppm): 1.18 (bs, 1H, CH_2), 1.47 (bs, 2H, CH_2), 1.68 (bs, 3H, CH_2), 2.47-2.84 (bs, 8H, 3x NCH_2 & CH_2), 3.77 (s, 3H, OCH_3), 4.11(bs, 2H, OCH_2), 6.33 (s, 2H, NH_2), 6.82 (s, 1H, ArH), 6.90 (d, 1H, *J* = 8.7 Hz, ArH), 6.99 (d, 2H, *J* = 8.1 Hz, ArH), 7.48 (d, 2H, *J* = 8.1 Hz, ArH), 8.07 (d, 1H, *J* = 8.4 Hz, ArH); ^{13}C NMR (DMSO-D_6, 75 MHz, δ ppm): 22.96, 23.96 (2xC), 24.65, 25.73, 28.89, 54.83 (2xC), 55.00, 56.09, 67.38, 113.42, 113.85, 114.70 (2C), 126.79 (2xC), 127.67, 131.09, 131.60, 142.19, 159.67, 160.62, 161.83, 162.85; ESIMS ($C_{25}H_{28}N_4O_2$): m/z = 417.5 $[M+H]^+$.

4-(4-(2-(dimethylamino)ethoxy)phenyl)-5,6-dihydro-8-methoxybenzo[h]quinazolin-2-amine (6c)

Off-white solid; R_f: 0.23 (10% methanol in chloroform); mp 114-116°C; IR (KBr, ν_{max}/cm^{-1}): 3318 (NH_2); ^1H NMR (DMSO-D_6, 300 MHz, δ ppm): 2.21 (s, 6H, 2xNCH_3), 2.48 (s, 2H, NCH_2), 2.62 (bs, 4H, 2xCH_2), 3.79 (s, 3H, OCH_3), 4.07(d, 1H, *J* = 4.8 Hz, OCH_2), 6.34 (s, 2H, NH_2), 6.83 (s, 1H, ArH), 6.90 (d, 1H, *J* = 7.8 Hz, ArH), 6.99 (d, 2H, *J* = 7.5 Hz, ArH), 7.49 (d, 2H, *J* = 6.9 Hz, ArH), 8.08 (d, 1H, *J* = 8.4 Hz, ArH); ^{13}C NMR (DMSO-D_6, 75 MHz, δ ppm): 24.65, 28.90, 46.40 (2xC), 56.10, 58.51, 66.75, 113.40, 113.53, 113.84, 114.68 (2xC), 126.81, 127.66, 131.08 (2xC), 131.55, 142.20, 159.75, 160.60, 161.82, 162.85, 164.75; ESIMS ($C_{23}H_{26}N_4O_2$): m/z = 391.5 $[M+H]^+$.

4-(4-(1-(dimethylamino)propan-2-yloxy)phenyl)-5,6-dihydro-8-methoxybenzo[h]quinazolin-2-amine (6d)

Off-white solid; R_f: 0.24 (10% methanol in chloroform); mp 104-106°C; IR (KBr, ν_{max}/cm^{-1}): 3318 (NH_2); ^1H NMR (DMSO-D_6, 300 MHz, δ ppm): 1.04 (d, 3H, *J* = 4.6 Hz, CH_3) (s, 6H, 2xNCH_3), 2.48 (s, 1H, NCH_2), 2.73 (bs, 4H, 2xCH_2), 2.91 (d, 1H, *J* = 5.1 Hz, NCH_2), 3.78 (s, 3H, OCH_3), 4.04(d, 1H, *J* = 4.8 Hz, OCH), 6.34 (s, 2H, NH_2), 6.83 (s, 1H, ArH), 6.90 (d, 1H, *J* = 7.8 Hz, ArH), 6.99 (d, 2H, *J* = 7.5 Hz, ArH), 7.49 (d, 2H, *J* = 6.9 Hz, ArH), 8.08 (d, 1H, *J* = 8.4 Hz, ArH); ^{13}C NMR (DMSO-D_6, 75 MHz, δ ppm): 24.66, 25.72, 28.90, 41.84(2xC), 46.75, 56.09, 58.40, 70.49, 113.40, 113.52, 113.83, 114.72, 115.60, 126.81, 127.66, 131.09, 131.55, 142.19, 159.85, 160.60, 161.82, 162.86, 164.75; ESIMS ($C_{24}H_{28}N_4O_2$): m/z : 405.5 $[M+H]^+$.

General procedure for the synthesis of compounds (8a-b)

Ethyl 4-(4-(2-amino-8-methoxy-5,6-dihydrobenzo[h]quinazolin-4-yl)phenoxy)butanoate (8a)

In a 100 mL round bottom flask, 4-(2-amino-5,6-dihydro-8-methoxybenzo[h]quinazolin-4-yl)phenol (**4a,** 319 mg, 1.00 mmol)) and was stirred in dimethylformamide (DMF, 9 mL) at 80°C. After five minutes, anhydrous K_2CO_3 (210 mg, 1.5 mmol) and substituted ethyl n-bromoalkanoate **7** (172 mg, 1.50 mmol) was added in reaction mixture and stirred the reaction for 5 h. The reaction mixture was poured in cold water with vigorous stirring and neutralized it with N/5 HCl solution. The precipitate was filtered and dried. The crude was purified by column chromatography with a mixture of chloroform-methanol (0.5 to 1.0%) to give the desired product **8a**.

Light yellow solid; R_f: 0.26 (30% acetone in hexane); mp 148-149 °C; IR (KBr, ν_{max}/cm^{-1}): 3474 (NH_2), 1728 (C=O) ; ^1H NMR (DMSO-d_6, 300 MHz, δ ppm): 1.67 (t, 3H, *J* = 6.9 Hz, CH_3), 1.97 (t, 2H, *J* = 6.9 Hz, CH_2), 2.45 (p, 2H, *J* = 7.2 Hz, CH_2), 2.72 (bs, 4H, 2xCH_2), 3.78 (s, 3H, OCH_3), 4.00 (m, 4H, 2xOCH_2), 6.31 (bs, 2H, NH_2), 6.88 (d, 1H, *J* = 2.1 Hz, ArH), 6.90 (d, 1H, *J* = 8.7 Hz, ArH), 6.98 (d, 2H, *J* = 8.7 Hz, ArH), 7.49 (d, 2H, *J* = 8.7 Hz, ArH), 8.08 (d, 1H, *J* = 8.7 Hz, ArH); ^{13}C NMR (DMSO-d_6, 75 MHz, δ ppm): 14.92, 24.61, 25.05, 28.86, 31.03, 56.08, 60.79, 67.46, 113.41, 113.52, 113.94, 114.67 (2xC) 126.72, 127.68, 131.07 (2xC), 131.53, 142.22, 159.71, 160.64, 161.85, 162.79, 164.75, 173.48; ESIMS ($C_{25}H_{27}N_3O_4$): m/z = 434.2 $[M+H]^+$.

Ethyl 5-(4-(2-amino-8-methoxy-5,6-dihydrobenzo[h]quinazolin-4-yl)phenoxy)pentanoate (8b)

Off white solid; R_f: 0.40 (30% acetone in hexane); mp 109-110 °C; ^1H NMR (DMSO-d_6, 300 MHz, δ ppm): 1.19 (t, 3H, *J* = 7.2 Hz, CH_3), 1.40 (bs, 4H, 2xCH_2), 2.38 (t, 2H, *J* = 6.9 Hz, CH_2), 2.77 (bs, 4H, 2xCH_2), 3.82 (s, 3H, OCH_3), 4.05 (m, 4H, 2xOCH_2), 6.34 (s, 2H, NH_2), 6.86 (s, 1H, ArH), 6.92 (d, 1H, *J* = 8.7 Hz, ArH), 7.01 (d, 2H, *J* = 8.4 Hz, ArH), 7.52 (d, 2H, *J* = 8.4 Hz, ArH), 8.11 (d, 1H, *J* = 8.4 Hz, ArH); ^{13}C NMR ($CDCl_3$, 75 MHz, δ ppm): 14.98, 22.07, 24.65, 28.86, 34.02, 35.00, 56.10, 60.59, 68.01, 113.41, 113.53, 113.85, 114.65 (2xC), 126.81, 127.66, 131.08 (2xC), 131.49, 142.20, 159.85, 160.59, 161.83, 162.86, 164.77, 173.65; ESIMS ($C_{26}H_{29}N_3O_4$): m/z = 448.2 $[M+H]^+$.

***In-vitro* Cancer Cell growth inhibition assay**

In vitro anticancer activity of synthesized compounds was studied by sulphorhodamine B (SRB) dye based plate assay. In brief, 10^4 cells per well were added in 96-well culture plates and incubated at 37 °C in 5% carbondioxide concentration. After overnight incubation of cells, serial dilutions of synthesized compound were added to the wells. Untreated cells served as control. After 48 h, cells were fixed with ice-cold tri-chloroacetic acid (50% w/v, 100 ml per well), stained with SRB (0.4% w/v in 1% acetic acid, 50 ml per well), washed and air-dried. Bound dye was solubilize with 10 mM tris base (150 ml per well) and absorbance was read at 540 nm on a plate reader. The cytotoxic effect of compound was calculated as % inhibition in cell growth as per formula: [1-(absorbance of drug treated cells/absorbance of untreated cells)x100]. Determination of IC_{50} (50% inhibitory concentration) was based on dose-response curves.

Tubulin polymerization assay

To a pre warmed 96 well plate, compounds were added at a conc of 10, 2, 0.4 and 0.08 µg/ml. Paclitaxel was used as a standard at a conc of 10µM.Tubulin protein provided in the kit was added to a pre prepared ice cold tubulin polymerization buffer [80mM PIPES pH 6.9, 2mM $MgCl_2$, 0.5mM EGTA] immediately before use and was kept on ice. The ratio at which tubulin protein is mixed with the tubulin polymerization buffer was as 200 µL of protein with 420µL of tubulin polymerization buffer that gave a final concentration of 3mg/mL tubulin in 80mM PIPES pH 6.9, 2mM $MgCl_2$, 0.5mM EGTA.

50 µL of this diluted tubulin solution was added to each well containing the treated compound at different concentration and immediately the plate was read at 37 °C with pre set kinetic parameters at 340 nm wavelength for a period of 60 min.

The increase in absorbance at the pre set Kinetic parameters (340 nm, 37 °C over 60 min period of time) is graphically obtained as the polymerization curve and the V_{max} values obtained by the Skanit software 4.0 are used to interpret the results for analyzing the effect of the compounds on the tubulin polymerization.

Cell cycle analysis

Cell cycle distribution was measured in concentration and time dependent manner by flow cytometric analysis of PI-stained cellular DNA, as described earlier. Briefly, MCF-7 cells (8 x 10^5 per well) were seeded in 60 mm tissue culture dishes and grown overnight (37 °C, 5% CO_2). Compound treated cells were harvested by trypsinization and fixed (30 min, 4°C) with ice-cold 70% ethanol at indicated time points. The pellets were washed

with PBS and re-suspended in a solution containing PI (20 µg/ml), Triton X100 (0.1%) and RNase (0.1mg/ml) in PBS. After incubation (45 min, in the dark, 37˚C), cells were analysed on a FACS Calibur flow cytometer (BD Biosciences). Distribution of cells in different phases of cell cycle was calculated using "Cell Quest" software.

Western blot assay

Cells were grown overnight in 60 mm tissue culture dishes and were exposed to vehicle and test molecule for 24 and 48 h at IC_{50} concentration. Cells were then harvested and lysed with M-PER reagent (Thermo Scientific) supplemented with protease and phosphatase inhibitors. After centrifugation at 12000 rpm, supernatant was collected and protein quantity was measured by BCA protein assay kit (Thermo Scientific). Equal amount of proteins (20 µg) were resolved in 8% SDS-PAGE, transferred onto PVDF membrane and probed overnight with anti-PARP (Cell Signaling Technolgy) and anti-actin (Sigma-Aldrich) antibodies. After incubation with HRP-conjugated secondary antibody for 1 h at room temperature, ECL solution (Bio-Rad) was added to the membrane and luminescence was detected by Chemidoc XRS+ system (Bio-Rad).

Ligand and protein preparation for docking experiments

The molecular docking of control inhibitors tamoxifen, colchicine and compounds **4a-f, 6a-d** and **8a-b** were executed by using software Autodock v 1.5.6 [23]. The 3.5 Å 3D crystallographic structure of estrogen receptor alpha & tubulin were retrieved through Brookhaven Protein DataBank (PDB) (http://www.pdb.org) (PDB ID: 3ERT and 4O2B). The ligand and receptor preparation was done by using Discovery studio v3.5 (Accelrys, Inc., San Diego, CA, USA). The receptor grid was generated using the ligands tamoxifen and colchicine co-crystallized in receptor. The standardization of software was done by redocking study of bound inhibitor. Visualization of the docked conformation was performed in pymol.

Acknowledgements

The authors thank the Director, CSIR-CIMAP and CSIR-CDRI for financial support. The work was carried out under project ChemBio (BSC-203) to AG and GAP 0115 (sponsored by DST, India) to JS. AS and FK acknowledge the Science & Engineering Research Board (SERB), Department of Science & Technology (DST), New Delhi, India for financial support through GAP-260 project (Sanction No.: SR/FT/LS-25/2010; 02/05/2012).

Notes and references

1. www.healthindia.com "Diseases & Conditions › World Cancer Day 2014: New cancer cases to increase five-fold by 2025".
2. R. Siegel, J. Ma, Z. Jou, A. Jemal, Cancer statistics 2014, CA *Cancer J. Clin*., 2014, **64**, 9.
3. http://www.who.int/mediacentre/factsheets/fs297/en/:Fact sheet N°297
4. K. l. Dao, R. N. Hanson, *Bioconjugate Chem.*, 2012, **23**, 2139.
5. J. D. Croxtall, K. McKeage, *Drugs*, 2011, **71**, 363.
6. A. E. wakeling, M. Dukes, J. Bowler, *Cancer Re*s., 1991, **51**, 3867.
7. A. Gupta, B. S. Kumar, A. S. Negi, *J. Steroid Biochem.,* 2013, **13**, 7242.
8. (a) J. Messinger, H. H. Thole, B. Husen, M. Weske, P. Koskimies, L, Pirkkala, U.S. Pat. Appl. Publ. 2006, US 20060281710 A1 20061214. (b) J. Messinger, H. H. Thole, B. Husen, M. Weske, P. Koskimies, L, Pirkkala, M. Weske, PCT Int. Appl. 2006, WO 2006125800 A1 20061130.
9. (a) C. V. Themsche, S. Parent, V. Leblanc, C. Descoteaux, A. M. Simard, G. Berube, E. Asselin, *Endocr. Rel. Can.* 2009, **16**, 1185. (b) K. Brasseur, V. Leblanc, F. Fabi, S. Parent, C. Descoteaux, G. Berube, E. Asselin, *Endocr.,* 2013, **154**, 2281.
10. G. M. Allan, C. Bubert, N. Vicker, A. Smith, H. J. Tutill, A. Purohit, M. J. Reed, B. V. L. Potter, *Mol. Cell. Endocr.,* 2006, **248**, 204.
11. A. Gupta, P. Saha, C. Descoteaux, V. Leblanc, E. Asselin, G. Berube, *Bioor. Med. Chem. Lett.,* 2010, **20**, 1614.
12. C. E. Geyer, J. Forster, D. Lindquist, S. Chan, C. G. Romieu, T. Pienkowski, A. Jagiello-Gruszfeld, J. Crown, A. Chan, B. Kaufman, D. Skarlos, M. Campone, N. Davidson, M. Berger, C. Oliva, S. D. Rubin, S. Stein, D. Cameron, *N. Engl. J. Med.* 2006, **355**, 2733.
13. E. Petit-Jean, T. Buclin, M. Guidi, E. Quoix, B. Gourieux, L. A. Decosterd, A-C. Gairard-Dory, G. Ubeaud-Séquier, N. Widmer, *Ther. Drug Monit.,* 2015, **37**, 2.
14. T. Araki, H. Yashima, K. Shimizu, T. Aomori, T. Hashita, K. Kaira, T. Nakamura, K. Yamamoto, *Clin. Med. Insights: Oncol.* 2012, 6407.
15. (a) S. Karras , P. Anagnostis, G. E. Krassas, *Expert Opin Drug Metab. Toxicol.* 2014, **10**, 469. (b) A. D. Luca, A. D'Alessio, M. R. Maiello, M. Gallo, S. Bevilacqua, D. Frezzetti, A. Morabito, F. Perrone, N. Normanno, *Expert. Opin. Investig. Drugs,* 2014, **23**, 1295.
16. H. K. Maurya, R. Verma, S. Alam, S. Pandey, V. Pathak, S. Sharma, K. K. Srivastava, A. S. Negi, A. Gupta, *Bioorg. Med. Chem. Lett.* 2013, **23**, 5844.
17. http://en.wikipedia.org/wiki/Choline.
18. C. Rub, B. Konig, *Green Chem.*, 2012, **14** 2969.
19. A. Zhu, T. Jiang, B. Han, J. Zhang, Y. Xie, X. Ma, *Green Chem.*, 2007, **9**, 169.
20. S. B. Phadtare, G. S. Shankarling, *Green Chem.*, 2010, **12**, 458.
21. P. Moriel, E. J. García-Suárez, M. Martínez, A. B. García, M. A. Montes-Morán, V. Calvino-Casilda, M. A. Bañares, *Tetrahedron Lett.,* 2010, **51**, 4877.
22. A. P. Abbott, G. Capper, D. L. Davies, R. K. Rasheed, V. Tambyrajah, *Green Chem.,* 2002, **4**, 24.
23. R. C. Morales, V. Tambyrajah, P. R. Jenkins, D. L. Davies, A. P. Abbott, *Chem. Commun.*, 2004, 158.
24. N. Azizi, E. Batebi, *Catal. Sci. Technol.*, 2012, **2**, 2445.
25. A. S. Negi, Y. Gautum, S. Alam, D. Chanda, S. Luqman, J. Sarkar, F. Khan, R. Konwar, *Bioorg. Med. Chem.,* 2015, **23**, 373.
26. S. W. Yu, S. A. Andrabi, H. Wang, N. S. Kim, G. G. Poirier, T. M. Dawson, V. L. Dawson, *Proc. Nat. Acad. Sci.,* 2006, **103**, 18314.

RSC Advances

Graphical Abstract:

Synthesis of 4-phenyl-5,6-dihydrobenzo[*h*]quinazolines and their evaluation as growth inhibitors of carcinoma cells

Hardesh K Maurya, Mohammad Hasanain, Sarita Singh, Jayanta Sarkar, Vijaya Dubey, Aparna Shukla, Suaib Luqman, Feroz Khan, Atul Gupta*

Synthesis of various benzo[*h*]quinazoline analogs (**4a-f, 6a-6d** and **8a-b**) was accomplished through the reaction of chalcone with guanidine. The synthesized compounds (**4a-f, 6a-6d & 8a-b**) were screened for their anticancer potential against different cancer cells *viz* MCF-7, DLD1, A549, Du145 & FaDu cell lines. Compounds **4a**, **6a-d** & **8b** showed significant anticancer activity in these cancer cell lines within the range of IC_{50} values of 1.5-12.99 µM. Functional study of a promising molecule, **6d,** at 7 µM **(**at IC_{50} value**)** for 24 and 48 h showed that it possessed anticancer activity through triggering apoptosis. In tubulin polymerization assay, **6d** effectively inhibited tubulin polymerization at IC_{50} 2.27 µM. *In-silico* docking study of **6d** revealed that **6d** had good affinity with estrogen receptor as well as tubulin protein on its β-sheet of colchicines binding site.